JACS Au
AN OPEN ACCESS JOURNAL OF THE AMERICAN CHEMICAL SOCIETY

pubs.acs.org/jacsau
Letter

Cyclic Peptides KS-133 and KS-487 Multifunctionalized Nanoparticles Enable Efficient Brain Targeting for Treating Schizophrenia

Kotaro Sakamoto,* Seigo Iwata, Zihao Jin, Lu Chen, Tatsunori Miyaoka, Mei Yamada, Kaiga Katahira, Rei Yokoyama, Ami Ono, Satoshi Asano, Kotaro Tanimoto, Rika Ishimura, Shinsaku Nakagawa, Takatsugu Hirokawa, Yukio Ago,* and Eijiro Miyako*

Cite This: JACS Au 2024, 4, 2811−2817

Read Online

ACCESS | Metrics & More | Article Recommendations | Supporting Information

ABSTRACT: Establishing drug delivery systems (DDSs) for transporting drugs from peripheral tissues to the brain is crucial for treating central nervous system diseases. We previously reported the interactions of (1) KS-133, a selective antagonist peptide, with vasoactive intestinal peptide receptor 2 (VIPR2), a drug target for schizophrenia, and (2) KS-487, a selective binding peptide, with the cluster IV domain of low-density lipoprotein receptor-related protein 1 (LRP1), which is involved in crossing the blood−brain barrier. We developed a novel DDS-based strategy for treating schizophrenia using KS-487 as a brain-targeting peptide and KS-133 as a drug. Dibenzocyclooctyne-KS-487 was conjugated with N_3-indocyanine green (ICG) using a click reaction and administered intravenously into mice. Fluorescence was clearly observed from ICG in the brains of the mice. Nanoparticles (NPs) encapsulating ICG and displaying KS-487 were prepared and subcutaneously administered to mice, resulting in a significant accumulation of ICG in the brain. Pharmacokinetic analysis of NPs containing KS-133 and displaying KS-487 (KS-133/KS-487 NPs) revealed the time-dependent transport of KS-133 into the brain. KS-133/KS-487 NPs were subcutaneously administered to mouse models of schizophrenia, which significantly improved cognitive dysfunction. This is the first study to demonstrate the potential therapeutic efficacy of a multifunctionalized multipeptide NP in inhibiting VIPR2.

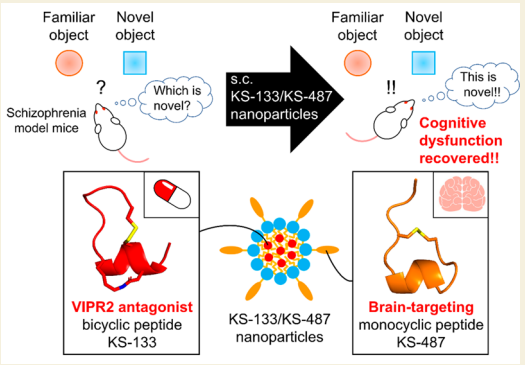

KEYWORDS: *Nanoparticles, Click chemistry, Peptides, Drug delivery, Schizophrenia*

The number of patients with central nervous system (CNS) diseases continues to increase every year globally, emphasizing the critical need for drug development in this field. However, developing drugs that target the CNS presents greater challenges than those that target peripheral tissues. The primary hurdle lies in the blood−brain barrier (BBB), a protective barrier that rigorously restricts the transfer of drug molecules from peripheral tissues to the brain.[1,2] The BBB specifically blocks middle-sized molecules, such as cyclic peptides, and macromolecules, including antibodies, making it exceedingly difficult for them to enter the brain. Many studies on DDSs have explored pathways that facilitate drug transport across the BBB into the brain.[3,4] One such pathway is receptor-mediated transcytosis (RMT) using low-density lipoprotein receptor-related protein 1 (LRP1),[5,6] which will be investigated in this study.

Among CNS diseases, the etiology and pathophysiology of schizophrenia, which is the focus of this study, are poorly understood. Several patients with schizophrenia do not adequately respond to current treatments. In 2011, a strong association was reported between vasoactive intestinal peptide receptor 2 (VIPR2) gene duplication and schizophrenia.[7,8] Therefore, VIPR2-selective inhibitors may aid the development of novel treatments for schizophrenia. In 2021, we discovered a peptide, KS-133: Ac-(CPPYLP[KYLC)D]LI-NH_2 (with an S−S bond between the side chains of Cys^1 and Cys^{10} and an amide bond between Lys^7 and Asp^{11}) as a VIPR2-selective antagonist, which suppresses the downstream signaling of VIPR2 in the brain.[9] However, developing KS-133 as an antischizophrenia drug was difficult because (1) KS-133 does not effectively penetrate the BBB and (2) there is no preclinical proof-of-concept demonstrating that VIPR2 inhibition improves symptoms in a mouse model of schizophrenia.

Received: April 5, 2024
Revised: May 31, 2024
Accepted: June 3, 2024
Published: June 20, 2024

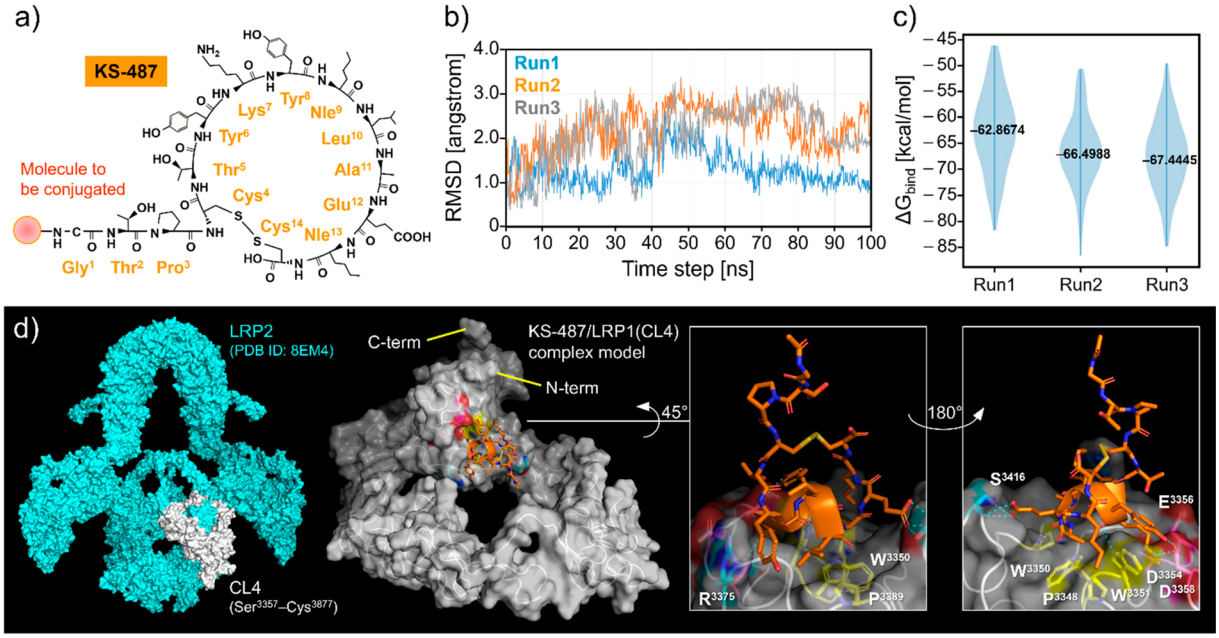

Figure 1. Construction of a KS-487/LRP1(CL4) complex model. a) Chemical structure of KS-487: Gly[1]-Thr[2]-Pro[3]-(Cys[4]-Thr[5]-Tyr[6]-Lys[7]-Tyr[8]-Nle[9]-Leu[10]-Ala[11]-Glu[12]-Nle[13]-Cys[14])−OH. b) The Cα atom root-mean-square deviations (RMSDs) of KS-487 on LRP1(CL4) complex models from the initial structure after the production phase in three runs are shown. c) Distribution of interaction energies in each run. d) Representative KS-487/LRP1(CL4) complex structure model (the most stable snapshot of run 3). To clearly indicate the CL4 (Ser[3332]−Asp[3779]) sequence on the LRP1 structure, CL4 (Ser[3357]−Cys[3877]) (white) of LRP2 (PDB ID: 8EM4) (light blue) is shown on the left. The complex structure model of LRP1(CL4) (gray ribbon) and KS-487 (ribbon and stick) are shown in the center. Cyan dash lines indicate hydrogen bond interaction. In LRP1(CL4), amino acids in yellow and cyan represent those engaged in hydrophobic and hydrophilic interactions with KS-487, respectively. The amino acids in pink are the acidic residues. The figure was generated using PyMOL.

To overcome these challenges, we combined KS-133 with a reliable brain-targeting technology.

In 2022, we discovered KS-487: Ac-GTP(CTYKY-Nle-LAE-Nle-C)−OH (with a S−S bond between the side chains of Cys[4] and Cys[14]) (Figure 1a) as a binding peptide to the cluster IV (CL4) domain (Ser[3332]−Asp[3779]) of LRP1. The permeability of this molecule across the BBB, as demonstrated using *in vitro* BBB models, could be diminished by siRNA against LRP1, suggesting that KS-487 crosses the *in vitro* BBB via RMT by LRP1.[10] Therefore, KS-487 is expected to have *in vivo* brain-targeting ability.

In this study, we developed a novel DDS by combining KS-487 with KS-133 to enhance brain permeability. Furthermore, we demonstrated, for the first time, that VIPR2 inhibition can treat schizophrenia. NPs that display KS-487 on the surface and encapsulate KS-133 can effectively transport from peripheral tissues to the brain, and their administration can improve cognitive function in a mouse model of schizophrenia.

The molecular mechanism underlying the interaction of KS-487 with LRP1 remains unknown. Through recent advancements in molecular structure prediction technologies, such as AlphaFold2 (AF2), complex molecular models can be developed with sufficient accuracy.[11,12] Previously, we successfully developed a complex model of VIPR2 and KS-133 using AF2 and molecular dynamics (MD) simulations, revealing the detailed binding mechanism.[13] Using the same technique, we attempted to elucidate the binding mechanism of KS-487 to LRP1(CL4). Initially, we considered predicting complex models of KS-487 and full-length LRP1 using the LRP2 structure,[14] which is structurally similar to LRP1. However, the number of amino acid residues in full-length LRP1 exceeded the limit supported by AF2 on the CollabFold server. Subsequently, we attempted to develop KS-487/LRP1(CL4) complex models and obtained an approved model by AF2. During the MD simulations (100 ns for 3 runs), the root-mean-square deviation (RMSD) values of each run remained stable between 1 and 3, indicating that the constructed KS-487/LRP1(CL4) complex models were highly accurate (Figure 1b). The average interaction energies were −62.8674 kcal/mol for run 1, − 66.4988 kcal/mol for run 2, and −67.4445 kcal/mol for run 3 (Figure 1c). Figure 1d shows the most stable KS-487/LRP1(CL4) complex structure obtained from run 3. KS-487 adopts a loop-helix structure, and the side chain of Tyr[6] engages in a stacking interaction with Arg[3375] of LRP1. The basic side chain of Lys[7] interacts with the acidic pocket of LRP1, which comprise Asp[3354], Glu[3356], and Asp[3358]. Moreover, the main chain oxygen of Lys[7] forms a hydrogen bond with the nitrogen of the side chain indole ring of Trp[3351]. The side chain of Tyr[8] establishes a hydrogen bond with Asp[3358] of LRP1. The hydrophobic interaction of the Leu[10] side chain with Pro[3389] of LRP1 spatially supports the side chain of Tyr[6], which facilitates the stacking interaction between Tyr[6] and Arg[3375]. The side chains of Ala[11] and Nle[13] engage in hydrophobic interactions to fill the space in the shallow groove comprising Pro[3348], Trp[3350], and Trp[3351] of LRP1. The side chain of Glu[12] forms hydrogen bonds with nitrogen and Ser[3416] from the main and side chains of LRP1, respectively. The N- and C-termini of KS-487 do not participate in LRP1 binding and are oriented toward the water-soluble side.

We used two approaches to design DDSs using KS-487 as the brain-targeting peptide. In the first approach, KS-487 was directly conjugated to the long-wavelength near-infrared (NIR) fluorescent dye ICG (775 g/mol). The second

https://doi.org/10.1021/jacsau.4c00311
JACS Au 2024, 4, 2811−2817

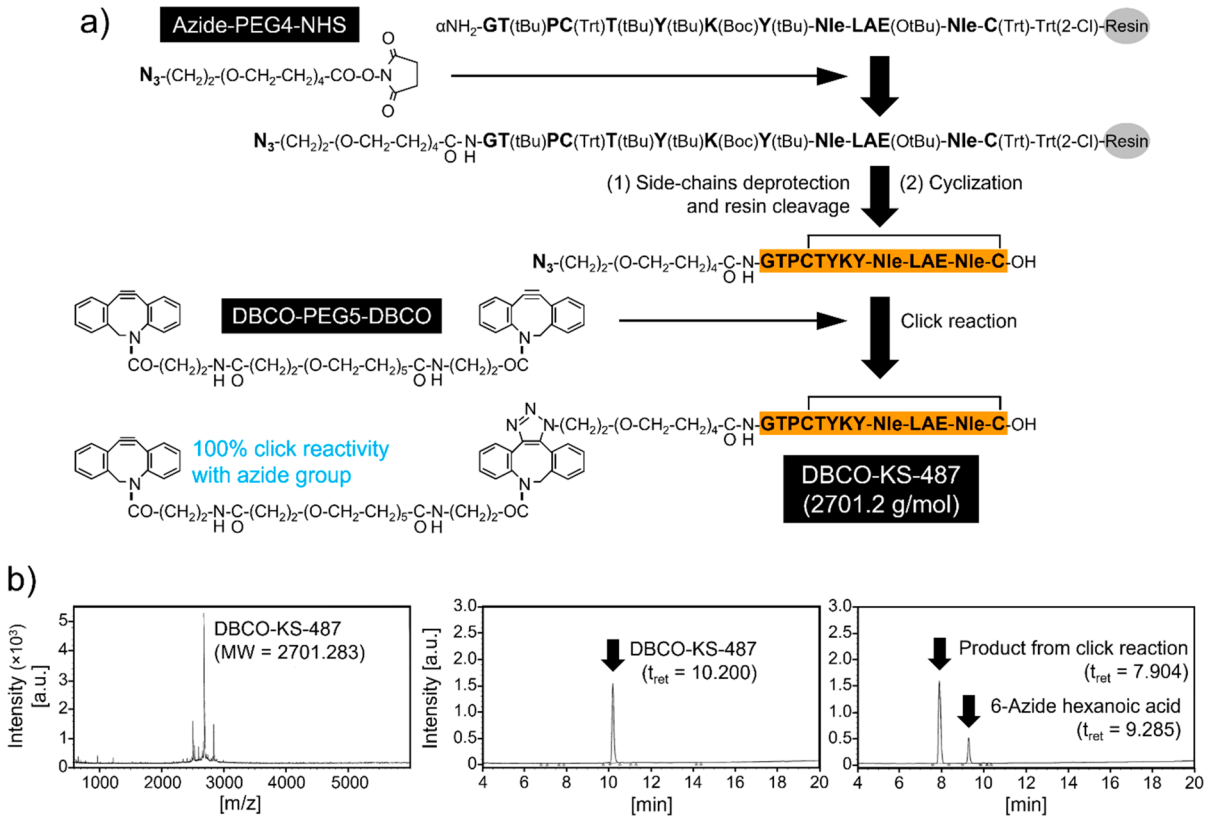

Figure 2. Molecular design and chemical synthesis of DBCO-KS-487. a) Preparation of DBCO-KS-487 using KS-487, azido-PEG4-NHS ester, and DBCO-PEG5-DBCO. b) Mass (left) and RP-HPLC (center) analytical data of DBCO-KS-487, and confirmation of the click reactivity of DBCO-KS-487 to 6-azide hexanoic acid as a model molecule possessing an azide group (right).

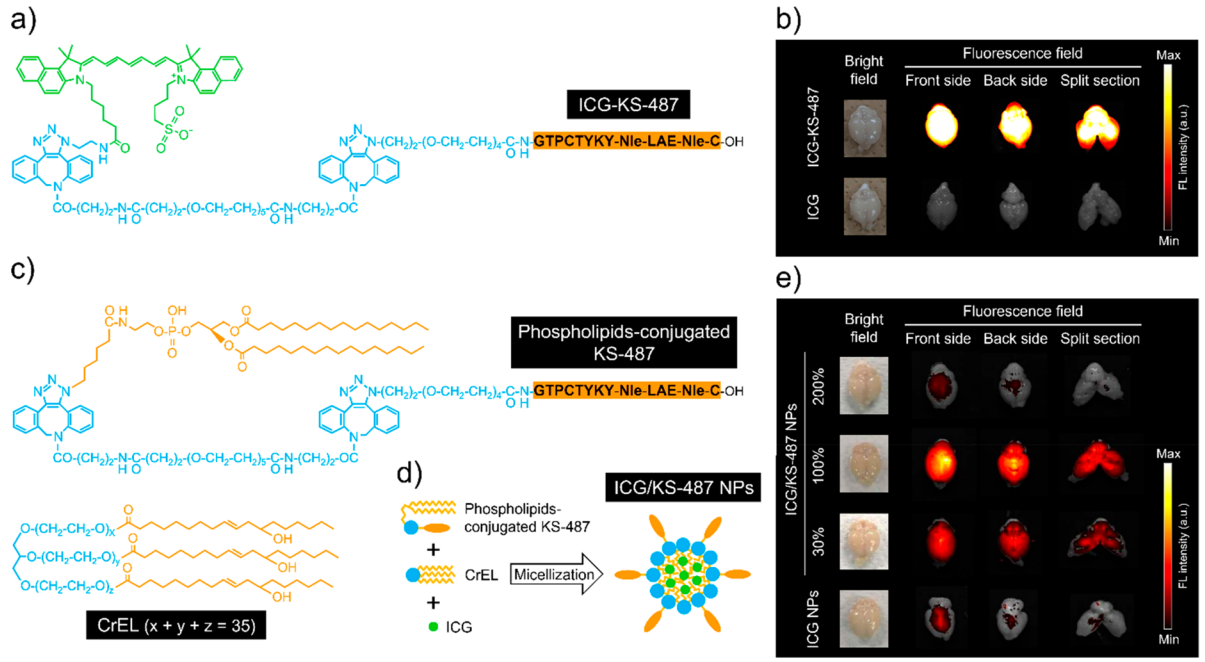

Figure 3. Evaluation of the brain-targeting ability of ICG-KS-487 and ICG/KS-487 NPs using bioimaging. a) Chemical structure of ICG-KS-487 prepared using DBCO-KS-487 and ICG azide. b) Brain-targeting ability of ICG-KS-487 (after 48 h of intravenous administration). c) Chemical structure of phospholipid-conjugated KS-487 prepared by DBCO-KS-487 and 16:0 azidocaproyl PE and chemical structure of CrEL. d) Schematic of NPs encapsulating ICG and displaying KS-487 (ICG/KS-487 NPs) by mixing phospholipids-introduced KS-487, CrEL and ICG. e) Brain-targeting ability of ICG/KS-487 NPs (after 48 h of subcutaneous administration). If the amount of KS-487 displayed on the surface of ICG/KS-487 NPs in the second row from the top is 100%, that in the top row is 200%, the third row is 30%, and the bottom row (ICG/NPs) has no KS-487 display (0%). ICG fluorescence was detected by setting the sensitivity of the instrument to values of 1,600−3,000 (fluorescence intensity a.u.).

https://doi.org/10.1021/jacsau.4c00311
JACS Au 2024, 4, 2811−2817

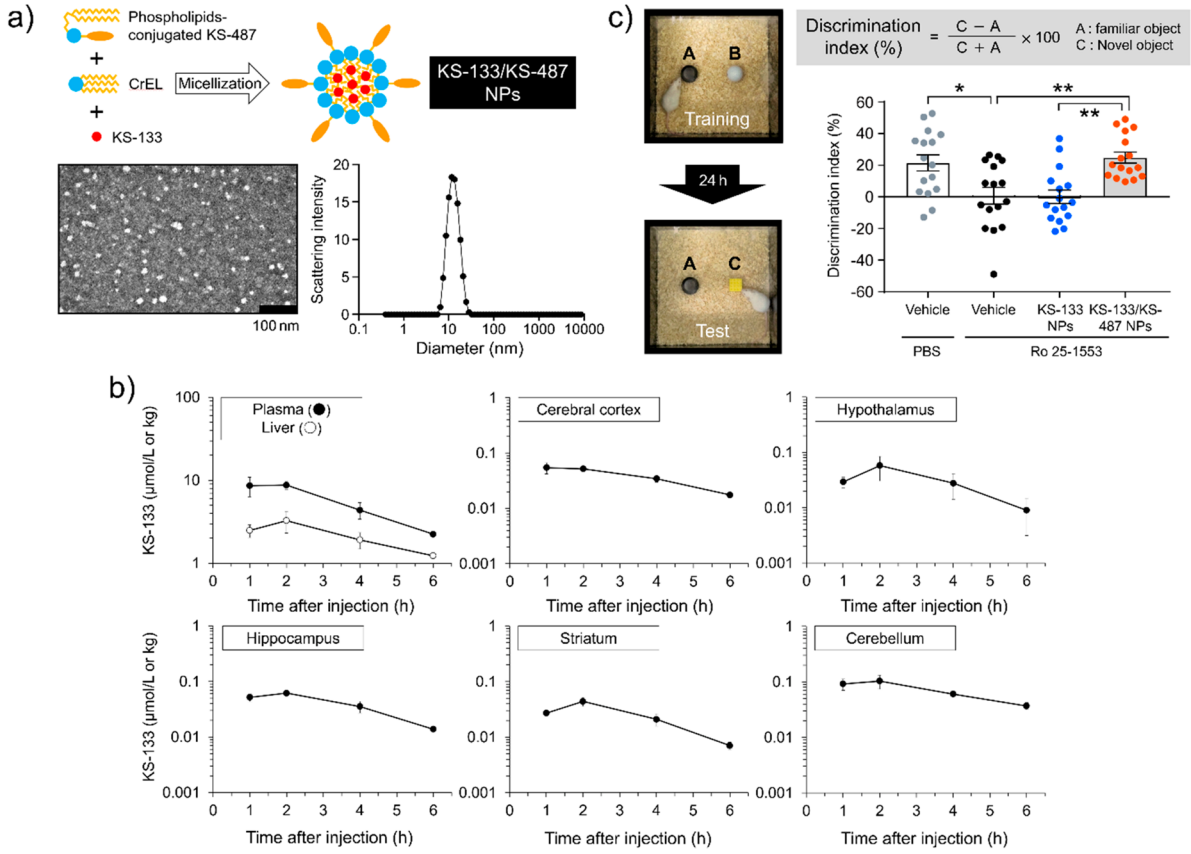

Figure 4. Pharmacokinetic study of KS-133/KS-487 NPs and pharmacological effects of KS-133/KS-487 NPs in a mouse model of schizophrenia. a) Upper panel: Schematic of NPs encapsulating KS-133 and displaying KS-487 (KS-133/KS-487 NPs) by mixing phospholipid-introduced KS-487, CrEL, and KS-133. Lower panel: Representative transmission electron microscopy analysis (left) (black bar = 100 nm) and representative size distribution (right) of KS-133/KS-487 NPs. b) Pharmacokinetics study of KS-133/KS-487 NPs subcutaneously administered in mice (n = 3 in each time point, mean ± SD, 3 mg/kg as a dose of KS-133). c) Left panel: Schematic of the novel objective recognition test. The VIPR2 agonist Ro 25−1553 was administered to mice to induce VIPR2 hyperactivation to create the mouse model of schizophrenia. Then, KS-133/KS-487 NPs (with a dose of 3 mg/kg KS-133) were administered once daily into the mice for 2 weeks. In the novel object recognition test, after training to remember objects A and B, object B was replaced by novel object C, and the exploration time to familiar object A and novel object C was evaluated. Right panel: Novel object recognition test results showing the effects of once daily subcutaneous administration of KS-133/KS-487 NPs on recognition memory. The discrimination index is calculated by the difference between the exploration time for novel and familiar objects divided by the total time spent exploring both objects. The results are presented as the mean ± SEM of 16 mice per group (*p < 0.05, **p < 0.01 by posthoc Tukey's multiple comparison test).

approach involved indirectly loading the therapeutic molecule, the VIPR2 antagonist KS-133 (1,558.8 g/mol), inside the micelles or liposomes that display KS-487. A straightforward method for conjugating KS-487 as a targeting peptide to specific molecules involves utilizing a click reaction, such as the one between a cyclooctyne group (e.g., DBCO) and an azide group (N_3). Initially, we considered introducing DBCO to the N-terminal amino group of KS-487 using DBCO-PEG4-NHS (CAS No. 127004-19-0). However, when DBCO was introduced at the N-terminal amino group with the side chain amino group of Lys^7 protected, followed by deprotection of the side chain of Lys^7, the click reactivity of DBCO was lost in a series of synthetic methods. Considering our prior experience in generating artificial receptor agonists through the synthesis of "peptide−linker−peptide" homodimers using bivalent reagents,[15,16] we attempted to synthesize "KS-487−linker−desired molecule" heterodimers using KS-487 with an azido group, a desired molecule that possesses an azido group, and the bivalent reagent DBCO-PEG5-DBCO. Consequently, we proposed introducing DBCO, maintaining click reactivity, into KS-487 through a click reaction between azide-introduced KS-487 and an excess amount of DBCO-PEG5-DBCO (Figure 2a). Therefore, we successfully synthesized DBCO-KS-487 with theoretical and actual molecular weights of 2,701.2 g/mol and 2,701.283 g/mol, respectively, and a purity of 97.2% (Figure 2b). DBCO-KS-487 and 6-azido-hexanoic acid were mixed in dimethyl sulfoxide (DMSO)/phosphate-buffered saline (PBS) (50/50) at pH 7.5 to an appropriate volume and reacted at room temperature; the peak position shift of DBCO-KS-487 was then evaluated using reversed-phase high-performance liquid chromatography (RP-HPLC) (Figure 2b). The peak (10.2 min) derived from DBCO-KS-487 before the reaction almost disappeared, and a new peak (7.904 min) was generated, indicating that the DBCO group of DBCO-KS-487 retains its activity for the click reaction.

For bioimaging analysis, ICG was conjugated to DBCO-KS-487 via a click reaction (Figure 3a). The LRP1-binding activity of ICG-KS-487 was confirmed by competitive binding assay (Figure S1). Subsequently, ICG alone or ICG-KS-487 was intravenously administered to mice, and the brains were

https://doi.org/10.1021/jacsau.4c00311
JACS Au 2024, 4, 2811−2817

harvested after 48 h. Fluorescence was clearly observed in the brains of mice treated with ICG-KS-487 but not in the brains of mice treated with ICG alone (Figure 3b), indicating that KS-487 exhibits robust *in vivo* brain-targeting ability. Next, we prepared NPs displaying KS-487 to develop a versatile brain-targeting DDS with KS-487. DBCO-KS-487 and azidated phospholipids (16:0 azidocaproyl PE) were mixed at weight ratios of 3:1, 1:1, and 0:1, and KS-487 was conjugated to the phospholipids using a click reaction at loading levels of approximately 100%, 30%, and 0% (Figure 3c). The LRP1-binding activity of phospholipids-conjugated KS-487 was confirmed by competitive binding assay (**Figure S1**). They were mixed with ICG and Cremophor EL (CrEL), an FDA-approved pharmaceutical additive, to prepare NPs encapsulating ICG, with or without displaying KS-487 (Figure 3d). Subsequently, these nanoparticles (NPs) were administered to mice through subcutaneous injection, and the brains were collected 48 h postadministration. As shown in Figure 3e, slight fluorescence was detected in the brains of mice treated with NPs encapsulating ICG; however, they did not display KS-487. In contrast, fluorescence was observed in the mouse brains treated with ICG/KS-487 NPs based on the amount of KS-487 displayed. Consequently, we prepared ICG/KS-487 NPs (200%), in which the amount of displayed KS-487 was increased using twice the amount of phospholipid-conjugated KS-487 and subjected to them the same test. The results showed that the transfer of ICG to the brain was reduced. These findings indicate that although NPs displaying KS-487 can deliver inclusions to the brain, the amount of KS-487 displayed on the surface of NPs should be optimal to achieve brain-targeting ability.

We investigated whether the VIPR2 antagonist KS-133 could be transported into the brain when encapsulated in NPs displaying KS-487. These NPs were prepared based on our previous report (Figure 4a).[17] KS-133 encapsulated in NPs composed of CrEL was stably retained at 4 °C but was gradually released from the NPs at 37 °C.[17] Transmission electron microscopy and particle size distribution analysis of KS-133/KS-487 NPs revealed monodisperse particles with diameters of approximately 12 nm (Figure 4a). The zeta potential of NPs composed solely of CrEL was −0.05 mV, and the zeta potential of NPs composed of CrEL and phospholipids-conjugated KS-487 was −6.37 mV.

A pharmacokinetic study was conducted to evaluate the time-dependent translocation of KS-133 in the brain after subcutaneous administration (3 mg/kg) of KS-133/KS-487 NPs (Figure 4b). The concentration of KS-133 in the plasma, liver, cerebral cortex, hypothalamus, hippocampus, striatum, and cerebellum was measured using liquid chromatography with tandem mass spectrometry (LC-MS/MS) at various time points (1, 2, 4, and 6 h). KS-133 concentrations in all tissues were consistent, peaking at 1−2 h after administration. The average maximum concentration was 8.734 μmol/L in the plasma, 3.265 μmol/kg in the liver, 0.054 μmol/kg in the cerebral cortex, 0.058 μmol/kg in the hypothalamus, 0.062 μmol/kg in the hippocampus, 0.044 μmol/kg in the striatum, and 0.103 μmol/kg in the cerebellum (Table 1). These data suggest that KS-133 is uniformly distributed throughout the brain. The peak concentration of KS-133 in the whole brain was estimated to be approximately 70 nM, which is sufficient for its antagonist activity (IC_{50} = 25 nM).

Finally, KS-133/KS-487 or KS-133 NPs (without KS-487) at 3 mg/kg doses were subcutaneously administered once daily for 2 weeks to a mouse model of schizophrenia induced by early postnatal treatment with a VIPR2 agonist Ro 25−1553, which were then subjected to the novel object recognition test.[9] Mice with good object recognition memory were expected to spend more time exploring the novel object than the familiar object during the retention session, thus the discrimination index is high. However, in schizophrenia model mice (Ro 25-1553/vehicle-treated group) impaired cognitive function, the discrimination index was significantly lower than PBS/vehicle-treated control group (Figure 4c). KS-133/KS-487 NPs-treated group, but not KS-133 NPs-treated group, showed a significant increase in discrimination index (Figure 4c). Therefore, cognitive dysfunction was improved in mice treated with KS-133/KS-487 NPs (Figure 4c), which can be attributed to VIPR2 inhibition by KS-133 transported to the brain.

Table 1. Pharmacokinetic Study of KS-133/KS-487 NPs[a]

Tissues	C_{max} (μmol/L or kg)	T_{max} (h)	$T_{1/2}$ (h)	AUC_{0-inf} (μmol/L× h)
Plasma	8.734	2	2.05	38.56
Liver	3.265	2	2.94	17.47
Cerebral cortex	0.054	1	2.38	0.28
Hypothalamus	0.058	2	1.35	0.19
Hippocampus	0.062	2	1.68	0.26
Striatum	0.044	2	1.38	0.15
Cerebellum	0.103	2	2.74	0.54

[a]NPs were subcutaneously administered in mice (Each value was calculated using the average concentration of the three animals at each time point. 3 mg/kg as a dose of KS-133).

In summary, our study successfully revealed the LRP1-binding mechanism of the cyclic peptide KS-487 and introduced a novel NP with significant brain-targeting capabilities, using KS-487. The combination of KS-133 with NPs represents a significant advancement in the development of KS-133 as a potential treatment for schizophrenia. KS-487 has emerged as a promising brain-targeting peptide for DDSs from peripheral tissues to the brain. In the future, KS-133/KS-487 NPs could be an effective treatment for schizophrenia, and KS-487 could advance drug development for refractory CNS diseases.

■ ASSOCIATED CONTENT

Data Availability Statement

All data needed to evaluate the conclusions in the paper are presented in the paper and/or Supporting Information. Additional data related to this paper are available from the corresponding author on reasonable request.

Supporting Information

The Supporting Information is available free of charge at https://pubs.acs.org/doi/10.1021/jacsau.4c00311.

Additional information on materials and methods and LRP1-binding activity of ICG-KS-487 and phospholipids-conjugated KS-487 (PDF)

■ AUTHOR INFORMATION

Corresponding Authors

Kotaro Sakamoto − *Research & Development Department, Ichimaru Pharcos Company Limited, Motosu 501-0475 Gifu, Japan*; Email: sakamoto-kotaro@ichimaru.co.jp

https://doi.org/10.1021/jacsau.4c00311
JACS Au 2024, 4, 2811−2817

Yukio Ago − *Laboratory of Biopharmaceutics, Osaka University, Suita 565-0871 Osaka, Japan; Department of Cellular and Molecular Pharmacology, Graduate School of Biomedical and Health Sciences, Hiroshima University, Hiroshima 734-8553, Hiroshima, Japan; Global Center for Medical Engineering and Informatics, Osaka University, Suita 565-0871 Osaka, Japan*; Email: yukioago@hiroshima-u.ac.jp

Eijiro Miyako − *Graduate School of Advanced Science and Technology, Japan Advanced Institute of Science and Technology, Nomi 923-1292 Ishikawa, Japan*; orcid.org/0000-0002-1157-6174; Email: e-miyako@jaist.ac.jp

Authors

Seigo Iwata − *Graduate School of Advanced Science and Technology, Japan Advanced Institute of Science and Technology, Nomi 923-1292 Ishikawa, Japan*

Zihao Jin − *Laboratory of Biopharmaceutics, Osaka University, Suita 565-0871 Osaka, Japan; Department of Cellular and Molecular Pharmacology, Graduate School of Biomedical and Health Sciences, Hiroshima University, Hiroshima 734-8553, Hiroshima, Japan*

Lu Chen − *Laboratory of Biopharmaceutics, Osaka University, Suita 565-0871 Osaka, Japan*

Tatsunori Miyaoka − *Laboratory of Biopharmaceutics, Osaka University, Suita 565-0871 Osaka, Japan*; orcid.org/0009-0003-7685-7780

Mei Yamada − *Laboratory of Biopharmaceutics, Osaka University, Suita 565-0871 Osaka, Japan*

Kaiga Katahira − *Laboratory of Biopharmaceutics, Osaka University, Suita 565-0871 Osaka, Japan*

Rei Yokoyama − *Department of Cellular and Molecular Pharmacology, Graduate School of Biomedical and Health Sciences, Hiroshima University, Hiroshima 734-8553, Hiroshima, Japan; Laboratory of Molecular Neuropharmacology, Osaka University, Suita 565-0871 Osaka, Japan*

Ami Ono − *Department of Cellular and Molecular Pharmacology, Graduate School of Biomedical and Health Sciences, Hiroshima University, Hiroshima 734-8553, Hiroshima, Japan; Department of Orthodontics and Craniofacial Developmental Biology, Graduate School of Biomedical and Health Sciences, Hiroshima University, Hiroshima 734-8553, Hiroshima, Japan*

Satoshi Asano − *Department of Cellular and Molecular Pharmacology, Graduate School of Biomedical and Health Sciences, Hiroshima University, Hiroshima 734-8553, Hiroshima, Japan*

Kotaro Tanimoto − *Department of Orthodontics and Craniofacial Developmental Biology, Graduate School of Biomedical and Health Sciences, Hiroshima University, Hiroshima 734-8553, Hiroshima, Japan*

Rika Ishimura − *Center for Supporting Drug Discovery and Life Science Research, Graduate School of Pharmaceutical Science, Osaka University, Suita 565-0871 Osaka, Japan*

Shinsaku Nakagawa − *Laboratory of Biopharmaceutics, Osaka University, Suita 565-0871 Osaka, Japan; Center for Supporting Drug Discovery and Life Science Research, Graduate School of Pharmaceutical Science, Osaka University, Suita 565-0871 Osaka, Japan; Global Center for Medical Engineering and Informatics, Osaka University, Suita 565-0871 Osaka, Japan*

Takatsugu Hirokawa − *Division of Biomedical Science, Institute of Medicine and Transborder Medical Research Center, University of Tsukuba, 305-8575 Tsukuba, Japan*; orcid.org/0000-0002-3180-5050

Complete contact information is available at: https://pubs.acs.org/10.1021/jacsau.4c00311

Author Contributions

▼S.I. and Z.J contributed equally to this work. CRediT: **Kotaro Sakamoto** conceptualization, data curation, formal analysis, funding acquisition, investigation, methodology, project administration, resources, writing-original draft, writing-review & editing; **Seigo Iwata** data curation, investigation; **Zihao Jin** data curation, investigation; **Lu Chen** validation; **Tatsunori Miyaoka** validation; **Mei Yamada** validation; **Kaiga Katahira** validation; **Rei Yokoyama** validation; **Ami Ono** validation; **Satoshi Asano** validation; **Kotaro Tanimoto** validation; **Rika Ishimura** validation; **Shinsaku Nakagawa** formal analysis, supervision; **Takatsugu Hirokawa** resources, software, validation; **Yukio Ago** formal analysis, funding acquisition, methodology, supervision, writing-review & editing; **Eijiro Miyako** conceptualization, data curation, formal analysis, funding acquisition, methodology, project administration, supervision, writing-original draft, writing-review & editing.

Notes

The authors declare the following competing financial interest(s): K.S. is a full-time employee of Ichimaru Pharcos Co. Ltd. The remaining authors declare that no competing interests are associated with this manuscript.

■ ACKNOWLEDGMENTS

We thank Yui Ikemi, Kazuto Nunomura, and Bangzhong Lin for their technical assistance with the experiments in the pharmacokinetic study. We also thank Dr. Daisuke Sugiyama (Translational Research Center, Hiroshima University, Hiroshima, Japan) for his advice on behavioral animal models to consider. This work was technically supported by the Platform Project for Supporting Drug Discovery and Life Science Research (Basis for Supporting Innovative Drug Discovery and Life Science Research (BINDS)) from the Japan Agency for Medical Research and Development (AMED, JP18am0101114, JP23ama121026j0002) and Research Support Project for Life Science and Drug Discovery (BINDS) from AMED under grant numbers JP23ama121052 and JP23ama121054. E.M. thanks the Japan Society for the Promotion of Science (JSPS) KAKENHI Grant-in-Aid for Scientific Research (A) (Grant number 23H00551), JSPS KAKENHI Grant-in-Aid for Challenging Research (Pioneering) (Grant number 22K18440), the Japan Science and Technology Agency for Adaptable and Seamless Technology Transfer Program through Target-driven R&D (Grant Number JPMJTR22U1), Institute for Fermentation, Osaka, and the Uehara Memorial Foundation. This work was partially supported by grants from JSPS KAKENHI to S.A. [23K091380] and Y.A. [20H03392, 24K02185] and Tokyo Biochemical Research Foundation in the form of a grant to Y.A. This research was also supported in part by AMED in the form of a grant to Y.A. [JP22ym0126809]. This work was partly supported by JST SPRING by a grant to A.O (JPMJSP2132) and SI (JPMJSP2102).

REFERENCES

(1) Sweeney, M. D.; Zhao, Z.; Montagne, A.; Nelson, A. R.; Zlokovic, B. V. Blood-brain barrier: From physiology to disease and back. *Physiol. Rev.* **2019**, *99*, 21−78.

(2) Choudhari, M.; Hejmady, S.; Narayan Saha, R.; Damle, S.; Singhvi, G.; Alexander, A.; Kesharwani, P.; Kumar Dubey, S. Evolving new-age strategies to transport therapeutics across the blood-brain-barrier. *Int. J. Pharm.* **2021**, *599*, 120351.

(3) Xie, J.; Shen, Z.; Anraku, Y.; Kataoka, K.; Chen, X. Nanomaterial-based blood-brain-barrier (BBB) crossing strategies. *Biomaterials* **2019**, *224*, 119491.

(4) Pinheiro, R. G R; Coutinho, A. J.; Pinheiro, M.; Neves, A. R. Nanoparticles for targeted brain drug delivery: What do we know? *Int. J. Mol. Sci.* **2021**, *22*, 11654.

(5) O'Sullivan, C. C.; Lindenberg, M.; Bryla, C.; Patronas, N.; Peer, C. J.; Amiri-Kordestani, L.; Davarpanah, N.; Gonzalez, E. M.; Burotto, M.; Choyke, P.; Steinberg, S. M.; Liewehr, D. J.; Figg, W. D.; Fojo, T.; Balasubramaniam, S.; Bates, S. E. ANG1005 for breast cancer brain metastases: correlation between ^{18}F-FLT-PET after first cycle and MRI in response assessment. *Breast Cancer Res. Treat.* **2016**, *160*, 51−59.

(6) Kumthekar, P.; Tang, S.-C.; Brenner, A. J.; Kesari, S.; Piccioni, D. E.; Anders, C.; Carrillo, J.; Chalasani, P.; Kabos, P.; Puhalla, S.; Tkaczuk, K.; Garcia, A. A.; Ahluwalia, M. S.; Wefel, J. S.; Lakhani, N.; Ibrahim, N. ANG1005, a brain-penetrating peptide-drug conjugate, shows activity in patients with breast cancer with leptomeningeal carcinomatosis and recurrent brain metastases. *Clin. Cancer Res.* **2020**, *26*, 2789−2799.

(7) Vacic, V.; McCarthy, S.; Malhotra, D.; Murray, F.; Chou, H.-H.; Peoples, A.; Makarov, V.; Yoon, S.; Bhandari, A.; Corominas, R.; Iakoucheva, L. M.; Krastoshevsky, O.; Krause, V.; Larach-Walters, V.; Welsh, D. K.; Craig, D.; Kelsoe, J. R.; Gershon, E. S.; Leal, S. M.; Aquila, M. D.; Morris, D. W.; Gill, M.; Corvin, A.; Insel, P. A.; McClellan, J.; King, M.-C.; Karayiorgou, M.; Levy, D. L.; DeLisi, L. E.; Sebat, J. Duplications of the neuropeptide receptor gene VIPR2 confer significant risk for schizophrenia. *Nature* **2011**, *471*, 499−503.

(8) Levinson, D. F.; Duan, J.; Oh, S.; Wang, K.; Sanders, A. R.; Shi, J.; Zhang, N.; Mowry, B. J.; Olincy, A.; Amin, F.; Cloninger, C R.; Silverman, J. M.; Buccola, N. G.; Byerley, W. F.; Black, D. W.; Kendler, K. S.; Freedman, R.; Dudbridge, F.; Pe'er, I.; Hakonarson, H.; Bergen, S. E.; Fanous, A. H.; Holmans, P. A.; Gejman, P. V. Copy number variants in schizophrenia: confirmation of five previous findings and new evidence for 3q29 microdeletions and VIPR2 duplications. *Am. J. Psychiatry* **2011**, *168*, 302−316.

(9) Sakamoto, K.; Chen, L.; Miyaoka, T.; Yamada, M.; Masutani, T.; Ishimoto, K.; Hino, N.; Nakagawa, S.; Asano, S.; Ago, Y. Generation of KS-133 as a novel bicyclic peptide with a potent and selective VIPR2 antagonist activity that counteracts cognitive decline in a mouse model of psychiatric disorders. *Front. Pharmacol.* **2021**, *12*, 751587.

(10) Sakamoto, K. Generation of KS-487 as a novel LRP1-binding cyclic peptide with higher affinity, higher stability and BBB permeability. *Biochem. Biophys. Rep.* **2022**, *32*, 101367.

(11) Varadi, M.; Anyango, S.; Deshpande, M.; Nair, S.; Natassia, C.; Yordanova, G.; Yuan, D.; Stroe, O.; Wood, G.; Laydon, A.; Žídek, A.; Green, T.; Tunyasuvunakool, K.; Petersen, S.; Jumper, J.; Clancy, E.; Green, R.; Vora, A.; Lutfi, M.; Figurnov, M.; Cowie, A.; Hobbs, N.; Kohli, P.; Kleywegt, G.; Birney, E.; Hassabis, D.; Velankar, S. AlphaFold protein structure database: Massively expanding the structural coverage of protein-sequence space with high-accuracy models. *Nucleic Acids Res.* **2022**, *50*, D439−D444.

(12) David, A.; Islam, S.; Tankhilevich, E.; Sternberg, M. J E The AlphaFold database of protein structures: A biologist's guide. *J. Mol. Biol.* **2022**, *434*, 167336.

(13) Sakamoto, K.; Asano, S.; Ago, Y.; Hirokawa, T. AlphaFold version 2.0 elucidates the binding mechanism between VIPR2 and KS-133, and reveals an S-S bond (Cys25-Cys192) formation of functional significance for VIPR2. *Biochem. Biophys. Res. Commun.* **2022**, *636*, 10−16.

(14) Beenken, A.; Cerutti, G.; Brasch, J.; Guo, Y.; Sheng, Z.; Erdjument-Bromage, H.; Aziz, Z.; Robbins-Juarez, S. Y.; Chavez, E. Y.; Ahlsen, G.; Katsamba, P. S.; Neubert, T. A.; Fitzpatrick, A. W P; Barasch, J.; Shapiro, L. Structures of LRP2 reveal a molecular machine for endocytosis. *Cell* **2023**, *186*, 821−836.

(15) Sakamoto, K.; Kawata, Y.; Masuda, Y.; Umemoto, T.; Ito, T.; Asami, T.; Takekawa, S.; Ohtaki, T.; Inooka, H. Discovery of an artificial peptide agonist to the fibroblast growth factor receptor 1c/βKlotho complex from random peptide T7 phage display. *Biochem. Biophys. Res. Commun.* **2016**, *480*, 55−60.

(16) Ohnishi, T.; Sakamoto, K.; Asami-Odaka, A.; Nakamura, K.; Shimizu, A.; Ito, T.; Asami, T.; Ohtaki, T.; Inooka, H. Generation of a novel artificial TrkB agonist, BM17d99, using T7 phage-displayed random peptide libraries. *Biochem. Biophys. Res. Commun.* **2017**, *483*, 101−106.

(17) Sakamoto, K.; Kittikulsuth, W.; Miyako, E.; Steeve, A.; Ishimura, R.; Nakagawa, S.; Ago, Y.; Nishiyama, A. The VIPR2-selective antagonist KS-133 changes macrophage polarization and exerts potent anti-tumor effects as a single agent and in combination with an anti-PD-1 antibody. *PLoS One* **2023**, *18*, e0286651.

https://doi.org/10.1021/jacsau.4c00311
JACS Au 2024, 4, 2811−2817